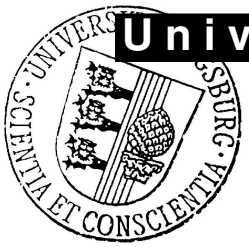

Universität Augsburg

Institut für Mathematik

Dirk Blömker, Christian Nolde, James Robinson

Rigorous Numerical Verification of Uniqueness and Smoothness in a Surface Growth Model

Preprint Nr. 16/2013 — 29. August 2013

Institut für Mathematik, Universitätsstraße, D-86135 Augsburg http://www.math.uni-augsburg.de/

Impressum:

Herausgeber:

Institut für Mathematik
Universität Augsburg
86135 Augsburg
`http://www.math.uni-augsburg.de/de/forschung/preprints.html`

ViSdP:

Dirk Blömker
Institut für Mathematik
Universität Augsburg
86135 Augsburg

Rigorous numerical verification of uniqueness and smoothness in a surface growth model

Dirk Blömker, Christian Nolde, James Robinson

August 20, 2013

Abstract

Based on numerical data and a-posteriori analysis we verify rigorously the uniqueness and smoothness of global solutions to a scalar surface growth model with striking similarities to the 3D Navier–Stokes equations, for certain initial data for which analytical approaches fail. The key point is the derivation of a scalar ODE controlling the norm of the solution, whose coefficients depend on the numerical data. Instead of solving this ODE explicitly, we explore three different numerical methods that provide rigorous upper bounds for its solution.

1 Introduction

We consider the following surface growth equation for the height $u(t,x) \in \mathbb{R}$ at time $t > 0$ over a point $x \in [0, 2\pi]$

$$\partial_t u(x,t) = -\partial_x^4 u(x,t) - \partial_x^2 \left(\partial_x u(x,t)\right)^2 \qquad x \in [0,2\pi],\ t \in [0,T] \tag{1}$$

with periodic boundary conditions and subject to a moving frame, which means $\int_0^{2\pi} u(x,t)\,\mathrm{d}x = 0$.

This equation, usually with additional noise terms, was introduced as a phenomenological model for the growth of amorphous surfaces [18, 16]. It was also used to describe sputtering processes [5]. See [3] for a detailed list of references. Based on the papers [4, 6, 17] which develop the theory of 'numerical verification of regularity' for the 3D Navier–Stokes equations, our aim here is to establish and implement numerical algorithms to rigorously prove global existence and uniqueness of solutions of (1).

Despite being scalar the equation has surprising similarities to 3D-Navier Stokes equations [1, 2, 3]. It allows for a global energy estimate in L^2 and

uniqueness of smooth local solutions in a largest critical space, with results for initial conditions being in a Besov-type space that contains C^0 or $H^{1/2}$, see [3] (similar results for the 3D Navier–Stokes equations can be found in [8]). Here we focus on the one-dimensional model, in order to have efficient and fast numerical methods available. For the two-dimensional case the situation seems even worse, as global existence could only be established in H^{-1} using the non-standard energy $\int_0^{2\pi} \mathrm{e}^{u(x)}\,\mathrm{d}x$. See [19] for details.

Rigorous numerical methods for proving numerically the existence of solutions for PDEs are a recent active research field. In addition to the approach taken here there are methods based on topological arguments like the Conley index, see [9, 7, 20], for example. For solutions of elliptic PDEs there are methods using Brower's fixed-point theorem, as discussed in the review article [15] and the references therein.

Our approach is based on [4] and similar to the method proposed by [12]. The key point is the derivation of a scalar ODE for the H^1-norm of the difference of an arbitrary approximation to the solution. The coefficients of this ODE depend only on the numerical data (or any other approximation used). As long as the solution of the ODE stays finite, one can rely on the continuation property of unique local solution, and thus have a smooth unique solution up to a blowup time of the ODE. A similar approach using an integral equation based on the mild formulation was proposed in [10, 11].

In order to establish a bound on the blow-up time for the ODE, one can either proceed analytically or numerically. We propose two analytical methods: one, based on the standard Gronwall Lemma, enforces a 'small data' hypothesis and adds little to standard analytical existence proofs. The second is based on an explicit analytical upper bound to the ODE solution. A variant of this, a hybdrid method in which one applies an analytical upper bound on a succession of small intervals of length $h > 0$ to the numerical solution and then restarts the argument, appears the most promising, and a formal calculation indicates that the upper bound from the third method in the limit of step-size to 0 converges to the solution of the ODE. In order to illustrate the three approaches, we use a spectral method with constant step-size and implicit discretization in time. For simplicity of presentation and of the numerical code, we assume that the numerical method actually provides a sufficiently good approximation of the true solution of the spectral method and proceed by ignoring errors in the residual due to time discretization. An extensive numerical study deriving rigorous (up to rounding errors) upper bounds is in preparation.

In order to derive the ODE for the H^1-error, we use a-priori estimates, where a crucial estimate is the linearized operator $Lv = -\partial_x^4 v + \partial_x^2(\partial_x\varphi \cdot \partial_x v)$ of the dynamics, given numerical data φ. In order to keep the method and

the numerical code simple, and as we can rely on the stability of the linear operator $-\partial_x^4$, we use here a type of worst case estimate by a-priori type estimates. An interesting approach in a slightly different context is proposed by [14, 13]. Here the spectrum of the linearized operator is analysed with a rigorous numerical method, which in case of an unstable linear operator yields substantially better results, at the price of a significantly higher computational time. This will be the subject of future research.

The paper is organized as follows. In Section 2 we establish the a-priori estimates for the H^1-error between solutions and the numerical data, that in the end gives an ODE depending on the numerical data only. Section 3 provides the ODE estimates necessary for our three methods, while Section 4 states the main results. In the final Section 5, we compare our methods using numerical experiments.

2 A priori analysis

In this section we establish upper bounds for the H^1-norm of the error

$$d(x,t) := u(x,t) - \varphi(x,t),$$

where u is a solution to our surface growth equation (1) and φ is any arbitrary, but sufficiently smooth approximation. Since we know φ, if we can control the H^1 norm of d then we control the H^1 norm of u.

For the following estimates and results, we define the H^p-norm, $p \geq 1$, of a function u by the seminorm

$$\|u\|_{H^p} := \|\partial_x^p u\|_{L^2}$$

which is equivalent to the standard H^p-norm as we only consider functions with vanishing mean, i.e. $\int_0^{2\pi} u(x,t)\,\mathrm{d}x = 0$. Further, the interval $[0, 2\pi]$ is denoted by Ω,

$$\Omega := [0, 2\pi].$$

2.1 Energy estimate

If we insert $d(x,t)$ into the surface growth equation (1) and use the residual of the approximation φ, given by

$$\mathrm{Res}(x,t) := \partial_t\varphi(x,t) + \partial_x^4\varphi(x,t) + \partial_x^2\left(\partial_x\varphi(x,t)\right)^2,$$

we have

$$\partial_t d = -\partial_x^4 d - \partial_x^2\left(\partial_x u\right)^2 + \partial_x^2\left(\partial_x\varphi\right)^2 - \mathrm{Res}$$

and by replacing u with $d - \varphi$ we finally get

$$\partial_t d = -\partial_x^4 d - \partial_x^2 \left(\partial_x d\right)^2 - 2\partial_x^2 \left(\partial_x d \cdot \partial_x \varphi\right)^2 - \mathrm{Res}\,.$$

For the H^1-norm we have

$$\begin{aligned}\frac{1}{2}\partial_t \|d(t)\|_{H^1}^2 = &\underbrace{\left\langle \partial_x^2 d(t), \partial_x^4 d(t)\right\rangle}_{\mathrm{A}} \\ &\underbrace{+ 2\int_0^{2\pi} \partial_x^2 \left(\partial_x d(x,t) \cdot \partial_x \varphi(x,t)\right) \cdot \partial_x^2 d(x,t)\,\mathrm{d}x}_{\mathrm{B}} \\ &\underbrace{+ \int_0^{2\pi} \partial_x^2 \left(\partial_x d(x,t)\right)^2 \cdot \partial_x^2 d(x,t)\,\mathrm{d}x}_{\mathrm{C}} \\ &\underbrace{+ \int_0^{2\pi} \mathrm{Res}(x,t) \cdot \partial_x^2 d(x,t)\,\mathrm{d}x,}_{\mathrm{D}}\end{aligned}$$

where $\langle \cdot, \cdot \rangle$ is the L^2 scalar product. Now consider these terms separately. First

$$\mathrm{A} = -\left\|\partial_x^3 d(t)\right\|_{L^2}^2 \qquad \text{int. by parts}$$

Secondly,

$$\begin{aligned}\mathrm{B} &= -2\int_0^{2\pi} \partial_x^3 d(x,t) \cdot \partial_x \left(\partial_x d(x,t) \cdot \partial_x \varphi(x,t)\right)\mathrm{d}x \\ &= \int_0^{2\pi} \left(\partial_x^2 d(x,t)\right)^2 \cdot \partial_x^2 \varphi(x,t)\,\mathrm{d}x \qquad \text{int. by parts} \\ &\quad -2\int_0^{2\pi} \partial_x^3 d(x,t) \cdot \partial_x d(x,t) \cdot \partial_x^2 \varphi(x,t)\,\mathrm{d}x\,.\end{aligned}$$

Thus

$$\begin{aligned}|\mathrm{B}| &\le \left\|\partial_x^2 d(t)\right\|_{L^2}^2 \left\|\partial_x^2 \varphi(t)\right\|_{L^\infty} \\ &\quad + 2\left\|\partial_x^3 d(t)\right\|_{L^2} \left\|\partial_x d(t)\right\|_{L^2} \left\|\partial_x^2 \varphi(t)\right\|_{L^\infty} \\ &\le 3\left\|\partial_x d(t)\right\|_{L^2} \left\|\partial_x^3 d(t)\right\|_{L^2} \left\|\partial_x^2 \varphi(t)\right\|_{L^\infty} \qquad \text{by interp.} \\ &\le \varepsilon \left\|d(t)\right\|_{H^3}^2 + \frac{9}{4\varepsilon}\left\|d(t)\right\|_{H^1}^2 \left\|\partial_x^2 \varphi(t)\right\|_{L^\infty}^2 \qquad \text{by Young ineq.}\end{aligned}$$

For C we have

$$\begin{aligned}\mathrm{C} &= -\int_0^{2\pi} \partial_x \left(\partial_x d(x,t)\right)^2 \cdot \partial_x^3 d(x,t)\,\mathrm{d}x \\ &= -2\int_0^{2\pi} \partial_x d(x,t)\cdot \partial_x^2 d(x,t)\cdot \partial_x^3 d(x,t)\,\mathrm{d}x\,.\end{aligned}$$

Thus

$$\begin{aligned}|\mathrm{C}| &\le 2\left\|\partial_x d(t)\right\|_{L^2}\left\|\partial_x^2 d(t)\right\|_{L^\infty}\left\|\partial_x^3 d(t)\right\|_{L^2} \\ &\le 2C_A\left\|\partial_x d(t)\right\|_{L^2}\left\|\partial_x^2 d(t)\right\|_{L^2}^{\frac{1}{2}}\left\|\partial_x^3 d(t)\right\|_{L^2}^{\frac{3}{2}} && \text{by Agmon ineq.} \\ &\le 2C_A\left\|\partial_x d(t)\right\|_{L^2}^{\frac{5}{4}}\left\|\partial_x^3 d(t)\right\|_{L^2}^{\frac{7}{4}} && \text{by interp.} \\ &\le \delta\left\|\partial_x^3 d(t)\right\|_{L^2}^2 + \frac{2^8\cdot C_A^8\cdot 7^7}{8\cdot 8^7\cdot\delta^7}\left\|\partial_x d(t)\right\|_{L^2}^{10} && \text{by Young ineq.} \\ &= \delta\left\|\partial_x^3 d(t)\right\|_{L^2}^2 + \underbrace{\frac{C_A^8\cdot 7^7}{4^8}}_{=:K}\cdot\frac{1}{\delta^7}\left\|\partial_x d(t)\right\|_{L^2}^{10}\end{aligned}$$

For the remaining term

$$\begin{aligned}|\mathrm{D}| &\le \left\|\mathrm{Res}(t)\right\|_{H^{-1}}\left\|\partial_x^3 d(t)\right\|_{L^2} \\ &\le \frac{\gamma}{2}\left\|\partial_x^3 d(t)\right\|_{L^2}^2 + \frac{1}{2\gamma}\left\|\mathrm{Res}(t)\right\|_{H^{-1}}^2 && \text{by Young ineq.}\end{aligned}$$

Summarizing the estimates we obtain

$$\begin{aligned}\frac{1}{2}\partial_t\|d(t)\|_{H^1}^2 \le &-\|d(t)\|_{H^3}^2\left(1-\varepsilon-\delta-\frac{\gamma}{2}\right)+\frac{K}{\delta^7}\left\|\partial_x d(t)\right\|_{L^2}^{10} \\ &+\frac{1}{2\gamma}\left\|\mathrm{Res}(t)\right\|_{H^{-1}}^2+\frac{9}{4\varepsilon}\|d(t)\|_{H^1}^2\left\|\partial_x^2\varphi(t)\right\|_{L^\infty}^2,\end{aligned}$$

where we can set $\varepsilon=\delta=\frac{1}{4}$ and $\gamma=\frac{1}{2}$ (all from Young's inequality) for simplicity

$$\begin{aligned}\frac{1}{2}\partial_t\|d(t)\|_{H^1}^2 \le &-\frac{1}{4}\|d(t)\|_{H^3}^2+K\cdot 4^7\left\|\partial_x d(t)\right\|_{L^2}^{10}+\left\|\mathrm{Res}(t)\right\|_{H^{-1}}^2 \\ &+9\|d(t)\|_{H^1}^2\left\|\partial_x^2\varphi(t)\right\|_{L^\infty}^2.\end{aligned}$$

In our setting we can use the optimal constants for Wirtinger's inequality (which is a special case of Poincaré inequality relevant to our setting), $\omega=1$, and Agmon's inequality, $C_A=1$ (and thus $K=7^7\cdot 4^{-8}$). Then we obtain

$$\begin{aligned}\frac{1}{2}\partial_t\|d(t)\|_{H^1}^2 \le &-\frac{1}{4}\|d(t)\|_{H^1}^2+\left\|\mathrm{Res}(t)\right\|_{H^{-1}}^2+\frac{7^7}{4}\|d(t)\|_{H^1}^{10} \\ &+9\left\|\partial_x^2\varphi(t)\right\|_{L^\infty}^2\|d(t)\|_{H^1}^2.\end{aligned} \tag{2}$$

This a scalar differential inequality of type

$$\begin{aligned}\xi'(t) &\le -c\cdot\xi(t) + f(t) + a(t)\cdot\xi(t) + b\cdot\xi(t)^5\\ &= b\cdot\xi(t)^5 + (a(t)-c)\cdot\xi(t) + f(t),\end{aligned} \tag{3}$$

and by standard ODE comparison principles a solution of the equality in (3) provides an upper bound for $\|d(t)\|_{H^1}^2$.

2.2 Time and smallness conditions

There are two important properties of the surface growth model that we want to use. These are the well known facts, also true for equations like Navier-Stokes, that smallness of the solution implies global uniqueness and that solutions are actually small after some time by energy type estimates.

First, if the H^1-norm of a solution u is smaller than some constant ε_0, we have global regularity of u. This is established by the same estimates derived for the parts (A) and (C) in Section 2.1. To be more precise:

$$\begin{aligned}\frac{1}{2}\partial_t\|u(t)\|_{H^1}^2 &= -\|\partial_x^3 u(t)\|_{L^2}^2 + \int_0^{2\pi}\partial_x^2\left(\partial_x u(x,t)\right)^2\cdot\partial_x^2 u(x,t)\,\mathrm{d}x\\ &\le -\|\partial_x^3 u(t)\|_{L^2}^2 + 2\,\|\partial_x u(t)\|_{L^2}\left\|\partial_x^2 u(t)\right\|_{L^\infty}\|\partial_x^3 u(t)\|_{L^2}\\ &= -\frac{3}{4}\|u(t)\|_{H^3}^2 + \frac{7^7}{4}\|u(t)\|_{H^1}^{10}\\ &\le -\frac{3}{4}\|u(t)\|_{H^1}^2 + \frac{7^7}{4}\|u(t)\|_{H^1}^{10} = \|u(t)\|_{H^1}^2\cdot\tfrac{1}{4}(7^7|u(t)\|_{H^1}^8 - 3)\end{aligned}$$

If $7^7\cdot\|u\|_{H^1}^8 \le 3$, then we obtain a global bound on $\|u\|_{H^1}^2$.

Theorem 1 (Smallness Condition)**.** *If for some $t\in[0,T]$ one has that $\|u\|_{H^1}$ is finite on $[0,t]$ and*

$$\|u(t)\|_{H^1} \le \left(\frac{3}{7^7}\right)^{\frac{1}{8}} =: \varepsilon_0,$$

then we have global regularity (and thus uniqueness) of the solution u on $[0,\infty)$.

Remark 2. Our crude estimate is $\varepsilon_0 \approx 0.209$. This is not too small, so we can use it numerically. But it is probably by far not optimal.

The second property is that, based on the smallness condition, we can determine a time T^*, only depending on the initial value $u(0)$, such that

$$\|u(\cdot,T^*)\|_{H^1} \le \varepsilon_0.$$

As an a-priori estimate we have

$$\partial_t \|u(t)\|_{L^2}^2 = -\left\|\partial_x^2 u(t)\right\|_{L^2}^2$$

and thus

$$\int_0^T \|\partial_x u(s)\|_{L^2}^2 \, \mathrm{d}s \leq \int_0^T \left\|\partial_x^2 u(s)\right\|_{L^2}^2 \, \mathrm{d}s \leq \|u(0)\|_{L^2}^2$$

where we used Poincaré inequality with constant $\omega = 1$. If we now assume that $\|\partial_x u(s)\|_{L^2} > \varepsilon_0$ for all $s \in [0, T]$, then

$$T\varepsilon_0^2 < \|u(0)\|_{L^2}^2 \quad \text{or} \quad T < \frac{1}{\varepsilon_0^2} \|u(0)\|_{L^2}^2$$

This means, that if we wait until time $T^* := \frac{\omega}{\varepsilon_0^2} \|u(0)\|_{L^2}^2$, we know that $\|\partial_x u(s)\|_{L^2} \leq \varepsilon_0$ for at least one $t \in [0, T^*]$ and we have global regularity by the smallness condition, if there was no blowup before time T^*.

Theorem 3 (Time Condition)**.** *If a solution u is regular up to time*

$$T^*(u(0)) := \frac{1}{\varepsilon_0^2} \|u(0)\|_{L^2}^2 = \left(\frac{7^7}{3}\right)^{\frac{1}{4}} \|u(0)\|_{L^2}^2 \,,$$

then we have global regularity of the solution u.

At the risk of labouring the point, we need only verify regularity of a solution start at $u(0)$ up to time $T^*(u(0))$, and from that point on regularity is automatic.

3 ODE estimates

We present several methods to bound ODEs of the type (2). In this section we give the results for the scalar ODE, and present applications in the next section. Let us first state a lemma of Gronwall type.

Lemma 4 (Gronwall)**.** *Let $a, b \in L^1([0, T], \mathbb{R})$ and $x \in W^{1,1}([0, T], \mathbb{R}) \cap C^0([0, T], \mathbb{R})$ such that*

$$x'(t) \leq a(t) \cdot x(t) + b(t) \qquad \forall t \in [0, T].$$

Then for all $t \in [0, T]$

$$x(t) \leq \exp\left(\int_0^t a(s) \, \mathrm{d}s\right) \cdot x(0) + \int_0^t \exp\left(\int_s^t a(r) \, \mathrm{d}r\right) \cdot b(s) \, \mathrm{d}s \,.$$

Now we prove a comparison theorem for a nonlinear differential inequality.

Lemma 5. *Consider two functions* $x, u \in W^{1,1}([0,T],\mathbb{R}^+) \cap C^0([0,T],\mathbb{R}^+)$ *such that*

$$x'(t) \le c(t)\cdot x(t)^p + e(t) \qquad x(0) = x_0$$

with $p > 1$, $c \in L^1([0,T],\mathbb{R}^+)$ *and* $e \in L^1([0,T],\mathbb{R}^+)$, *and let* u *be the solution of*

$$u'(t) = c(t)\cdot u(t)^p \qquad u(0) = x_0 + \int_0^T e(s)\,\mathrm{d}s.$$

Then $x(t) \le u(t)$ *for all* $t \in [0,T]$.

Proof. First note that if $e \equiv 0$ on $[0,T]$ then by using the standard comparison principle it follows that $u(t) \ge x(t)$ for all $t \in [0,T]$.

So now we assume that $\int_0^T e(s)\,\mathrm{d}s > 0$. For a contradiction, suppose that there exists a time $t^* \in [0,T]$ such that $t^* := \inf\{t > 0 : x(t) = u(t)\}$. Because of the continuity of $u(t)$ and $x(t)$, and $u(0) > x(0)$ due to our initial assumption $\int_0^T e(s)\,\mathrm{d}s > 0$, it follows that $t^* > 0$. From the definition $u(t) > x(t)$ for all $t \in [0,t^*)$, and thus

$$\begin{aligned} 0 = u(t^*) - x(t^*) &\ge u(0) - x(0) - \int_0^{t^*} e(s)\,\mathrm{d}s \\ &+ \int_0^{t^*} c(s)\left(u(s)^p - x(s)^p\right)\,\mathrm{d}s \\ &= \underbrace{\int_{t^*}^T e(s)\,\mathrm{d}s}_{\ge 0} + \int_0^{t^*} c(s)\,\underbrace{\left(u(s)^p - x(s)^p\right)}_{>0}\,\mathrm{d}s \end{aligned}$$

This yields the required contradiction provided that $\int_0^{t^*} c(s)\,\mathrm{d}s > 0$.

If $\int_0^{t^*} c(s)\,\mathrm{d}s = 0$, then as $c \ge 0$ we obtain

$$x(t) \le x(0) + \int_0^t e(s)\,\mathrm{d}s \le x(0) + \int_0^T e(s)\,\mathrm{d}s = u(t) \quad \forall t \in [0,t^*],$$

and we can repeat the above argument on the interval $[t^*,T]$ to obtain a contradiction. □

Now we can solve for $u(t)$. As $\mathrm{d}u = c(t)\,\mathrm{d}t$, a straightforward calculation verifies

$$u(t) = u(0)\cdot\left(1 - (p-1)\cdot u(0)^{p-1}\cdot\int_0^t c(s)\,\mathrm{d}s\right)^{-\frac{1}{p-1}}$$

as long as the right hand side is finite. Thus for all $t \in [0,T]$, as long as the right hand side is finite,

$$\begin{aligned} x(t) \leq & \left(x_0 + \int_0^T e(s)\,\mathrm{d}s\right) \\ & \cdot \left(1 - (p-1)\Big[x_0 + \int_0^T e(s)\,\mathrm{d}s\Big]^{p-1} \cdot \int_0^t c(s)\,\mathrm{d}s\right)^{-\frac{1}{p-1}} \end{aligned}$$

This holds especially if $T = t$. We finally obtain the following theorem:

Theorem 6 (CP-Type I)**.** *Assume $x \in W^{1,1}([0,T],\mathbb{R}^+) \cap C^0([0,T],\mathbb{R}^+)$ such that*

$$x'(t) \leq c(t) \cdot x(t)^p + e(t) \qquad x(0) = x_0$$

with $p > 1$, $c \in L^1([0,T],\mathbb{R}^+)$ and $e \in L^1([0,T],\mathbb{R}^+)$.

Then for all $t \in [0,T]$, as long as the right hand side is finite,

$$x(t) \leq \left(x_0 + \int_0^t e(s)\,\mathrm{d}s\right)\left(1 - (p-1)\cdot\Big[x_0 + \int_0^t e(s)\,\mathrm{d}s\Big]^{p-1} \cdot \int_0^t c(s)\,\mathrm{d}s\right)^{-\frac{1}{p-1}}.$$

We now extend this result to differential inequalities of type

$$x'(t) \leq b(t) \cdot x(t)^p + a(t) \cdot x(t) + f(t),$$

where $p > 1$, $f, b \in L^1([0,T],\mathbb{R}^+)$ and $a \in L^1([0,T],\mathbb{R})$. If we consider the substitution $y(t) = \mathrm{e}^{-A(t)} \cdot x(t)$ with $A(t) = \int_0^t a(s)\,\mathrm{d}s$, it follows that

$$\begin{aligned} y'(t) &= -a(t) \cdot y(t) + \mathrm{e}^{-A(t)} \cdot x'(t) \\ &\leq -a(t) \cdot y(t) + \mathrm{e}^{-A(t)} \cdot (b(t) \cdot x(t)^p + a(t) \cdot x(t) + f(t)) \\ &= \underbrace{b(t) \cdot \mathrm{e}^{(p-1)A(t)}}_{\tilde{b}(t)} \cdot y(t)^p + \underbrace{\mathrm{e}^{-A(t)} \cdot f(t)}_{\tilde{f}(t)} \end{aligned}$$

with $\tilde{b}(t) > 0$ and $\tilde{f}(t) > 0$ for all $t \in [0,T]$. Here we can apply Theorem 6 and obtain

$$y(t) \leq \left(y_0 + \int_0^t \tilde{f}\,\mathrm{d}s\right) \cdot \left(1 - (p-1) \cdot \Big[y_0 + \int_0^t \tilde{f}\,\mathrm{d}s\Big]^{p-1} \cdot \int_0^t \tilde{b}\,\mathrm{d}s\right)^{-\frac{1}{p-1}}.$$

Now substitute back with $x(t) = \mathrm{e}^{A(t)} \cdot y(t)$ and we finally derive the following corollary.

Corollary 7 (CP-Type II). *Assume* $x \in W^{1,1}([0,T],\mathbb{R}^+) \cap C^0([0,T],\mathbb{R}^+)$ *such that*

$$x'(t) \le b(t)\cdot x(t)^p + a(t)\cdot x(t) + f(t),$$

with $p>1$, $b, f \in L^1([0,T],\mathbb{R}^+)$ *and* $a \in L^1([0,T],\mathbb{R})$.

Then for all $t\in[0,T]$, *as long as the right hand side is finite,*

$$\begin{aligned} x(t) \le\ & \mathrm{e}^{A(t)}\cdot\Big(x_0 + \int_0^t \tilde f(s)\,\mathrm{d}s\Big) \\ & \cdot\Big(1+(1-p)\cdot\Big[x_0+\int_0^t \tilde f(s)\,\mathrm{d}s\Big]^{p-1}\cdot\int_0^t \tilde b(s)\,\mathrm{d}s\Big)^{\frac{1}{1-p}} \end{aligned}$$

where

$$\tilde b(t) = b(t)\cdot \mathrm{e}^{(p-1)A(t)},\quad \tilde f(t) = \mathrm{e}^{-A(t)}\cdot f(t),\quad \textit{and}\quad A(t)=\int_0^t a(s)\,\mathrm{d}s\,.$$

4 Verification methods

We now outline three techniques for numerical verification. The first is based on the simple Gronwall Lemma 4, the second on Corollary 7, and the third is similar but restarts the estimation after a series of short time-steps.

4.1 First method

If we take a closer look at the inequality (2), we see that as long as

$$\frac{7^7}{4}\,\|d(t)\|_{H^1}^8 \le \frac{1}{8}, \tag{4}$$

we obtain

$$\begin{aligned} \partial_t\|d(t)\|_{H^1}^2 \le & -\frac{1}{4}\|d(t)\|_{H^1}^2 + 2\|\operatorname{Res}(t)\|_{H^{-1}}^2 \\ & + 18\,\|d(t)\|_{H^1}^2\,\big\|\partial_x^2\varphi(t)\big\|_{L^\infty}^2\,. \end{aligned}$$

Now we can apply Lemma 4 and get the following estimate:

$$\begin{aligned} \|d(t)\|_{H^1}^2 \le\ & \|d(0)\|_{H^1}^2\cdot\exp\Big\{-\frac{t}{4}+18\int_0^t\|\partial_x^2\varphi(\tau)\|_{L^\infty}^2\mathrm{d}\tau\Big\} \\ & + 2\int_0^t \|\operatorname{Res}(s)\|_{H^{-1}}^2\cdot\exp\Big\{-\frac{t-s}{4}+18\int_s^t\|\partial_x^2\varphi(\tau)\|_{L^\infty}^2\,\mathrm{d}\tau\Big\}\mathrm{d}s \end{aligned}$$

Now we can use this bound to verify the initial guess (4), and we obtain the following theorem.

Theorem 8. *As long as*

$$\|d(0)\|_{H^1}^2 \cdot \mathrm{e}^{A(t)} + 2\int_0^t \|\operatorname{Res}(s)\|_{H^{-1}}^2 \cdot \mathrm{e}^{(A(t)-A(s))}\,\mathrm{d}s \le \left(7^7 \cdot 2\right)^{-\frac{1}{8}}, \quad (5)$$

we have

$$\|d(t)\|_{H^1}^2 \le \|d(0)\|_{H^1}^2 \cdot \mathrm{e}^{A(t)} + 2\int_0^t \|\operatorname{Res}(s)\|_{H^{-1}}^2 \cdot \mathrm{e}^{(A(t)-A(s))}\,\mathrm{d}s$$

where $A(t) = -\frac{1}{4}t + 18\int_0^t \|\partial_x^2\varphi(\tau)\|_{L^\infty}^2\,\mathrm{d}\tau$.

Note that the condition in (5) involves only the numerical solution φ.

4.2 Second method

The second way to obtain an upper bound for $\|d(t)\|_{H^1}^2$ is to apply Corollary 7 (CP-Type II) to our inequality (2). The corresponding functions are

$$b(t) = \frac{7^7}{4}, \quad a(t) = 9 \cdot \left\|\partial_x^2\varphi(t)\right\|_{L^\infty}^2 - \frac{1}{4}, \quad f(t) = \|\operatorname{Res}(t)\|_{H^{-1}}^2$$

and we immediately get the following theorem:

Theorem 9. *As long as the right hand side is finite*

$$\begin{aligned}\|d(t)\|_{H^1}^2 \le \mathrm{e}^{A(t)} &\cdot \left(\|d(0)\|_{H^1}^2 + \int_0^t \tilde{f}(s)\,\mathrm{d}s\right) \\ &\cdot \left(1 - 4 \cdot \left[\|d(0)\|_{H^1}^2 + \int_0^t \tilde{f}(s)\,\mathrm{d}s\right]^4 \cdot \int_0^t \tilde{b}(s)\,\mathrm{d}s\right)^{-1/4}\end{aligned}$$

with

$$\tilde{b}(t) = \frac{7^7}{4} \cdot \mathrm{e}^{4\cdot A(t)}, \qquad \tilde{f}(t) = \mathrm{e}^{-A(t)} \cdot \|\operatorname{Res}(t)\|_{H^{-1}}^2$$

and

$$A(t) = -\frac{1}{4} \cdot t + \int_0^t 9 \cdot \left\|\partial_x^2\varphi(s)\right\|_{L^\infty}^2\,\mathrm{d}s.$$

Again, the condition for regularity provided by the theorem depends only on the numerical solution φ.

4.3 Second method with restarting

The previous method can be further improved by introducing something that can be best described as "restarting". Instead of estimating over the whole time interval $[0, T]$ at once, we estimate to some smaller t^* and use the resulting upper bound as the new initial value.

Given some arbitrary partition $\{t_i\}_{0 \le i \le n}$ of the interval $[0, T]$ with $t_0 = 0$ and $t_n = T$, we define our new method as follows.

First, we apply Theorem 9 to the interval $[0, t_1]$

$$\begin{aligned} z(0) &:= \|d(0)\|_{H^1}^2 \\ \|d(t_1)\|_{H^1}^2 &\le \mathrm{e}^{A(t_1)} \cdot \left(z(0) + \int_0^{t_1} \tilde{f}(s)\, \mathrm{d}s \right) \\ &\quad \cdot \left(1 - 4 \cdot \left[z(0) + \int_0^{t_1} \tilde{f}(s)\, \mathrm{d}s \right]^4 \cdot \int_0^{t_1} \tilde{b}(s)\, \mathrm{d}s \right)^{-1/4} \\ &=: z(t_1) \end{aligned}$$

and define the upper bound for $\|d(t_1)\|_{H^1}^2$ as $z(t_1)$. In the next step, $z(t_1)$ is taken as the new "initial value" when we apply Theorem 9 to the interval $[t_1, t_2]$.

$$\begin{aligned} \|d(t_2)\|_{H^1}^2 &\le \mathrm{e}^{A(t_2)} \cdot \left(z(t_1) + \int_{t_1}^{t_2} \tilde{f}(s)\, \mathrm{d}s \right) \\ &\quad \cdot \left(1 - 4 \cdot \left[z(t_1) + \int_{t_1}^{t_2} \tilde{f}(s)\, \mathrm{d}s \right]^4 \cdot \int_{t_1}^{t_2} \tilde{b}(s)\, \mathrm{d}s \right)^{-1/4} \end{aligned}$$

where $\tilde{b}(t), \tilde{f}(t)$ are defined as before, only $A(t)$ for $t \in (t_{i-1}, t_i]$ changes to

$$A(t) = -\frac{1}{4} \cdot (t - t_{i-1}) + \int_{t_{i-1}}^{t} 9 \cdot \left\| \partial_x^2 \varphi(s) \right\|_{L^\infty}^2 \, \mathrm{d}s.$$

In summary we have the following.

Theorem 10. *Given any arbitrary partition $\{t_i\}_{0 \le i \le n}$ of the interval $[0, T]$ with $t_0 = 0$ and $t_n = T$, then by Theorem 9 we have for all $1 \le i \le n$*

$$\begin{aligned} z(0) &:= \|d(0)\|_{H^1}^2 \\ \|d(t_i)\|_{H^1}^2 &\le \mathrm{e}^{A(t_i)} \cdot \left(z(t_{i-1}) + \int_{t_{i-1}}^{t_i} \tilde{f}(s)\, \mathrm{d}s \right) \\ &\quad \cdot \left(1 - 4 \cdot \left[z(t_{i-1}) + \int_{t_{i-1}}^{t_i} \tilde{f}(s)\, \mathrm{d}s \right]^4 \cdot \int_{t_{i-1}}^{t_i} \tilde{b}(s)\, \mathrm{d}s \right)^{-1/4} \\ &=: z(t_i) \end{aligned}$$

as long as the right hand side is finite, where for $t \in (t_{i-1}, t_i]$

$$\tilde{b}(t) = \frac{7^7}{4} \cdot \mathrm{e}^{4 \cdot A(t)}, \qquad \tilde{f}(t) = \mathrm{e}^{-A(t)} \cdot \|\mathrm{Res}(t)\|_{H^{-1}}^2$$

and

$$A(t) = -\frac{1}{4} \cdot (t - t_{i-1}) + \int_{t_{i-1}}^{t} 9 \cdot \|\partial_x^2 \varphi(s)\|_{L^\infty}^2 \, \mathrm{d}s.$$

Let us give an informal argument that this method converges to a solution of the ODE as $h \to 0$. Let $z(t)$ be a smooth interpolation of the discrete points $z(t_i)$, $i = 1, 2, \ldots.$ with $t = t_j$. Then

$$\partial_t z(t_j) \approx \frac{z(t_{j+1}) - z(t_j)}{h}$$

Using, $\int_{t_j}^{t_{j+1}} g \, \mathrm{d}s \approx g(t_j)h$ and the abbreviation $z(t_j) = z_j$, we obtain from Theorem 10

$$\partial_t z(t_j) \approx \frac{1}{h}\Big[\frac{\mathrm{e}^{A_{j+1}}(z_j + h\tilde{f}_j)}{(1 - 4[z_j + h\tilde{f}_j]^4 h\tilde{b}_j)^{1/4}} - z_j\Big]$$

Using $\tilde{b}_j = \frac{7^7}{4}\mathrm{e}^{4A_j}$ and $\tilde{f}_j = \mathrm{e}^{-A_j}\,\mathrm{Res}_j = \mathrm{Res}_j$, as $A_j = 0$ yields

$$\begin{aligned}
\partial_t z(t_j) &\approx \frac{1}{h}\Big[\frac{\mathrm{e}^{A_{j+1}}(z_j + h\,\mathrm{Res}_j)}{(1 - [z_j + h\,\mathrm{Res}_j]^4 \cdot h7^7)^{1/4}} - z_j\Big] \\
&\approx \frac{1}{h}\Big[\frac{\mathrm{e}^{A_{j+1}} z_j + h\mathrm{e}^{A_{j+1}}\,\mathrm{Res}_j - z_j\sqrt[4]{1 - 7^7 h[z_j + h\,\mathrm{Res}_j]^4}}{\sqrt[4]{1 - 7^7 h[z_j + h\,\mathrm{Res}_j]^4}}\Big] \\
&\approx \frac{1}{h}\Big[\mathrm{e}^{A_{j+1}} z_j + h\mathrm{e}^{A_{j+1}}\,\mathrm{Res}_j - z_j\sqrt[4]{1 - 7^7 h[z_j + h\,\mathrm{Res}_j]^4}\Big]
\end{aligned}$$

Now using $\sqrt[4]{1-x} \approx 1 - \frac{1}{4}x + O(x^2)$

$$\begin{aligned}
\partial_t z(t_j) &\approx \mathrm{e}^{A_{j+1}}\,\mathrm{Res}_j + \frac{1}{h}(\mathrm{e}^{A_{j+1}} - 1)z_j + z_j\frac{1}{4}7^7[z_j + h\,\mathrm{Res}_j]^4 \\
&\approx \mathrm{Res}_j + A'(t_j)z_j + \frac{1}{4}7^7 z_j^5
\end{aligned}$$

using, that $A_{j+1} = O(h)$. Recall that $\mathrm{Res}_j = \|\,\mathrm{Res}(t_j)\|_{H^{-1}}^2$. Moreover, from the definition of $A'(t_j) = -\frac{1}{4} + 9\|\partial_x^2\varphi(t_j)\|_{L^\infty}^2$ and we thus recover that z solves (2) with equality in the limit $h \to 0$.

5 Numerical examples

To perform numerical verification rigorously, upper bounds for the three methods need to be calculated that include rounding errors (e.g using interval arithmetic). However, as our aim here is to illustrate the general behaviour and feasibility of the three methods, we neglected the rounding error and even made some simplifying assumptions to the residual in order to prevent the numerical code of getting too complex.

For our simulations we calculated an approximate solution using a spectral Galerkin scheme in space and a semi-implicit Euler scheme with stepsize h in time, yielding the values $\varphi(t)$ for $t = 0, h, 2h, ...$

A simple and straightforward way to show global regularity for initial data u_0 is to reach time $T^*(u_0)$ (from Theorem 3) with one of the methods outlined in the previous section. In the example presented in Figure 4 reaching T^* is just a matter of time. Getting below ε_0 with the norm of φ plus error seems to be rather hard in most of the cases.

For simplicity of the examples we always assume that $\varphi : [0, T] \to P_N L^2$ is actually the true solution of the spectral Galerkin method, i.e.

$$\partial_t \varphi = -\partial_x^4 \varphi - \partial_x^2 P_N (\partial_x \varphi)^2,$$

where P_N is the projection onto the first N Fourier-modes. Thus the residual simplifies to

$$\mathrm{Res}(\varphi) = (I - P_N)\partial_x^2 (\partial_x \varphi)^2,$$

which should be a very good approximation for sufficiently small h. (Under the *assumption* of regularity one can prove that the Galerkin approximations will converge to the true solution, which can be used to show that 'numerical verification' will be successful if the solution is indeed regular, see [4, 6], for example.) The following four figures should give an intuition of the differences and similarities of the three methods when changing the initial value or the residual directly.

It is not the purpose of the numerical examples to actually reach T^* and show global regularity. Especially, as T^* is a rough upper bound.

In Figure 1 we set the number of Fourier-modes intentionally small, in order to have a large residual. We can see that method 1 fails quite fast at approximately $T = 0.03$ by growing above the threshold, whereas methods 2 and 3 stay bounded for longer times and yield essentially identical bounds.

In Figure 2 we present the result with more Fourier-modes and therefore a smaller residual. Method 2 and 3 decreased from order 10^{-4} to order 10^{-18} but again they both appear to be basically the same, but now also method 1 stays below the threshold. Note, that the threshold is not shown in Figure

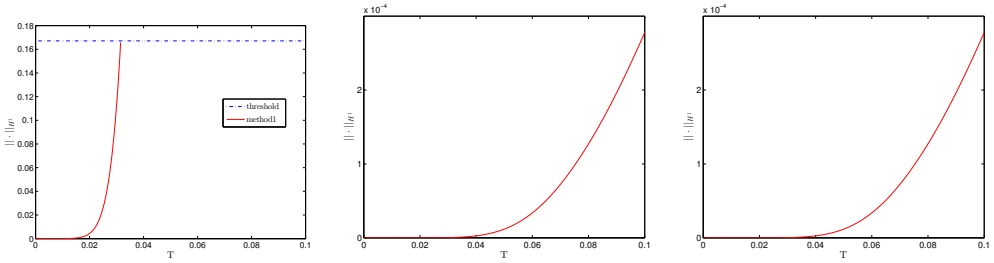

(a) Method 1 (b) Method 2 (c) Method 3

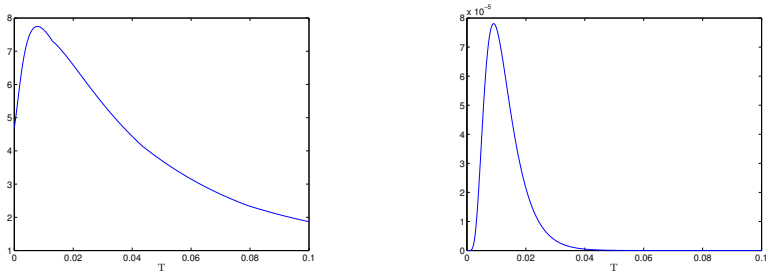

(d) $\|\partial_x^2\varphi\|_{L^\infty}$ (e) $\|\operatorname{Res}\|_{H^{-1}}$

Figure 1: Early failure of the first method and nearly identical behaviour for method 2 and 3 for initial value $u(0) = \cos(x) + \sin(2x)$, few Fourier modes $N = 64$, and small step-size $h = 10^{-6}$.

2a because its value of approximately 0.17 is so much larger than the bound with an order of 10^{-4}.

In the numerical approximation $\|\partial_x^2\varphi\|_{L^\infty}$ stays roughly the same as before, and it seems that the code approximates well the true solution. The residual decreased from magnitude 10^{-5} to 10^{-12} because we doubled the number of Fourier-modes. So as expected, the smaller residual decreased the bounds which are delivered by all 3 methods, what is especially important for method 1 as it is not valid above a certain threshold. Nevertheless, in this example even method 2 and 3 do fail with a finite-time blow-up, as soon as the bound gets to the order of magnitude of the threshold of method 1.

In Figure 3 we illustrate the differences between the methods 2 and 3. For this, we want to have a (relative) large residual and a smaller second derivative $\|\partial_x^2\varphi\|_{L^\infty}$. For example, in Figure 1 the residual is of order 10^{-5}, whereas the second derivative is of order 1. Unfortunately, due to our spectral Galerkin method we were not able produce a large residual without having a large second derivative. So, in order to show the main differences we artificially set $\|\partial_x^2\varphi\|_{L^\infty}$ and $\|\operatorname{Res}(t)\|_{H^{-1}}$ as constant, without using any

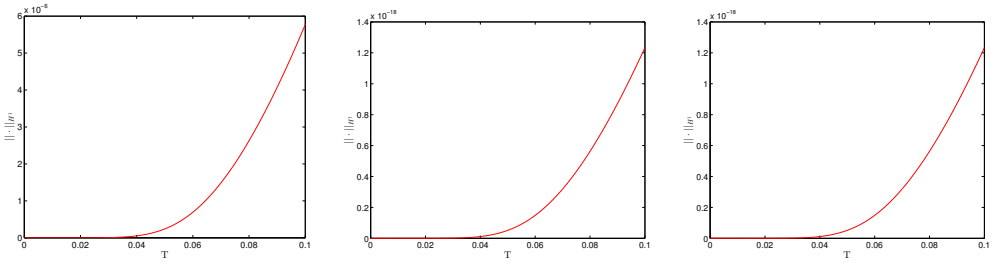

(a) Method 1 (b) Method 2 (c) Method 3

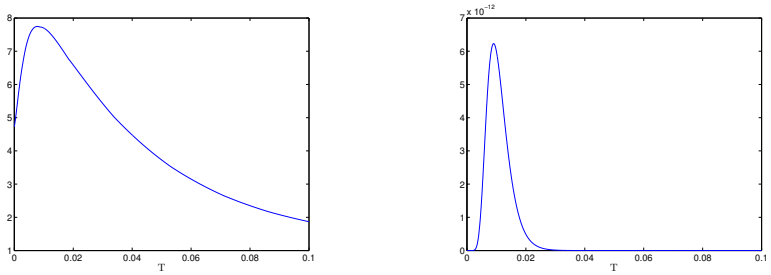

(d) $\|\partial_x^2 \varphi\|_{L^\infty}$ (e) $\|\operatorname{Res}\|_{H^{-1}}$

Figure 2: Improved Approximation by taking more Fourier modes. Note that the scale of (a) is shrunk by a factor 10^{-12} compared to (b) and (c). $u(0) = \cos(x) + \sin(2x)$, $N = 128$ and $h = 10^{-6}$

numerical approximation. Figure 3 shows, that in this case method 3 delivers the largest time interval as it stays finite up to $T \approx 0.16$, whereas method 2 has a blowup at $T \approx 0.11$ and method 1 at $T \approx 0.03$.

Figure 4 is just a small example to show that it is possible to reach the time T^* with these methods. The bounds of all three methods are already decreasing because the second derivative and the residual are sufficiently small (Again, the critical threshold for method 1 is not shown in the figure as it is too large). Now reaching T^* is only a matter of time, and we do not give the full graph up to T^*.

6 Conclusion

We presented a method to rigorously verify global existence and uniqueness by combining a-posteriori numerical data and a-priori estimates, which yields a differential inequality for the error from the data to the true solution having coefficients depending only on data. Three methods are presented to evaluate analytic upper bounds for the error from these differential inequalities.

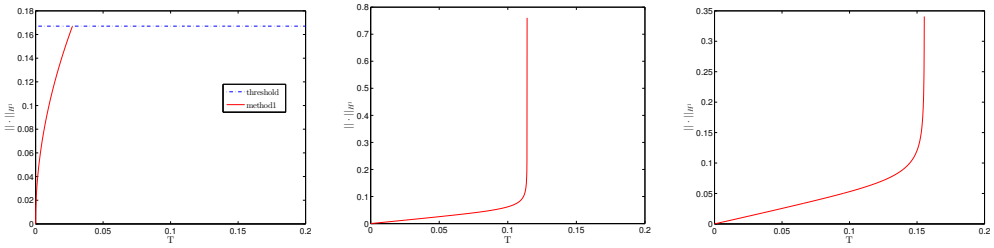

(a) Method 1 (b) Method 2 (c) Method 3

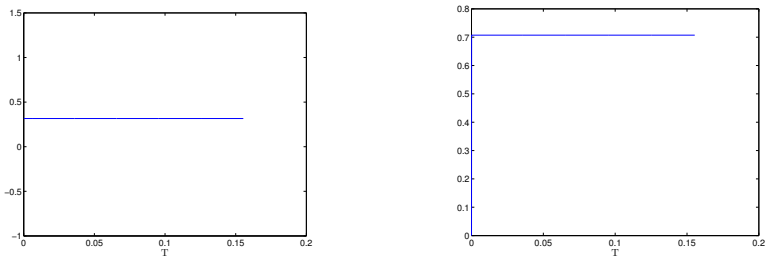

(d) $\|\partial_x^2 \varphi\|_{L^\infty}$ (e) $\|\,\mathrm{Res}\,\|_{H^{-1}}$

Figure 3: Artificial example for large fixed residual and not too large second derivative. Method 3 is superior, but all methods do blow up relatively fast, as the residual is large.

The third method seems to be the best method, as it provides rigorous upper bounds and converges to a solution of the equality in the differential inequality. Nevertheless, in all practical examples with our Galerkin approximation, method 2 and 3 yield nearly indistinguishable results.

While our implementation of the verification methods are not completely rigorous, our analysis and computations suggest that numerical verification of regularity is feasible and able to obtain global existence for initial conditions that are not covered by analytical results.

We plan to perform a fully rigorous numerical verification in a future paper, taking into account the errors in the Galerkin method and using interval arithmetic to keep track of truncation errors. Moreover, replacing the a-priori estimates of the linearized operator by rigorous numerical estimates for its spectrum looks promising.

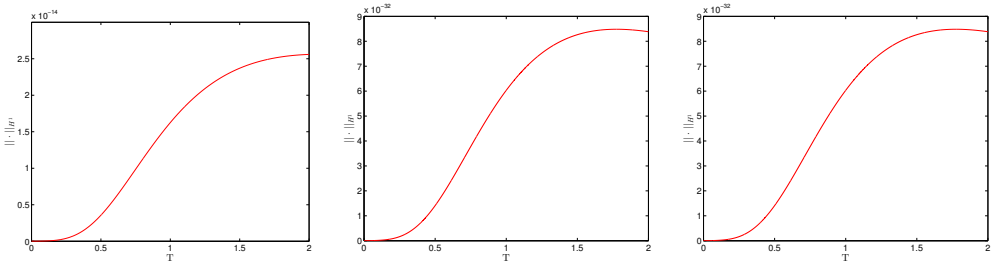

(a) Method 1 (b) Method 2 (c) Method 3

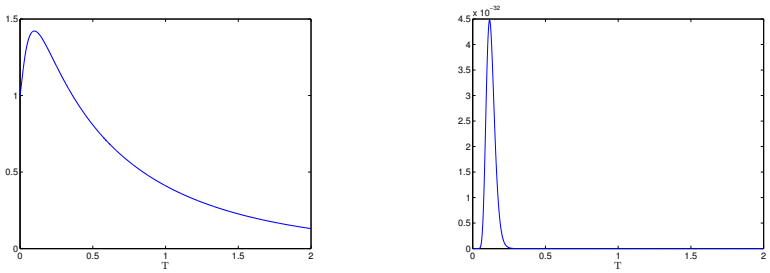

(d) $\|\partial_x^2 \varphi\|_{L^\infty}$ (e) $\|\operatorname{Res}\|_{H^{-1}}$

Figure 4: Example for possible global regularity for $u(0) = \sin(x)$. The error starts to decrease and remains bounded for long times. The figure focuses on the initial phase, and the result up to $T^* \approx 71,9$ is not shown.

References

[1] Dirk Blömker, Franco Flandoli, and Marco Romito. Markovianity and ergodicity for a surface growth PDE. *Ann. Probab.*, 37(1):275–313, 2009.

[2] Dirk Blömker and Marco Romito. Regularity and blow up in a surface growth model. *Dyn. Partial Differ. Equ.*, 6(3):227–252, 2009.

[3] Dirk Blömker and Marco Romito. Local existence and uniqueness in the largest critical space for a surface growth model. *NoDEA, Nonlinear Differ. Equ. Appl.*, 19(3):365–381, 2012.

[4] Sergei I. Chernyshenko, Peter Constantin, James C. Robinson, and Edriss S. Titi. A posteriori regularity of the three-dimensional Navier-Stokes equations from numerical computations. *J. Math. Phys.*, 48(6):065204, 15 p., 2007.

[5] R. Cuerno, L. Vázquez, and R. Gago. Self-organized ordering of nanostructures produced by ion-beam sputtering. *Phys. Rev. Lett.*, 94:016102, 4 p., 2005.

[6] Masoumeh Dashti and James C. Robinson. An a posteriori condition on the numerical approximations of the Navier-Stokes equations for the existence of a strong solution. *SIAM J. Numer. Anal.*, 46(6):3136–3150, 2008.

[7] Sarah Day, Jean-Philippe Lessard, and Konstantin Mischaikow. Validated continuation for equilibria of PDEs. *SIAM J. Numer. Anal.*, 45(4):1398–1424, 2007.

[8] H. Koch and D. Tataru. Well-posedness for the Navier-Stokes equations. *Adv. Math.*, 157(1):22–35, 2001.

[9] Stanislaus Maier-Paape, Ulrich Miller, Konstantin Mischaikow, and Thomas Wanner. Rigorous numerics for the Cahn-Hilliard equation on the unit square. *Rev. Mat. Complut.*, 21(2):351–426, 2008.

[10] Carlo Morosi and Livio Pizzocchero. On approximate solutions of semilinear evolution equations. II: Generalizations, and applications to Navier-Stokes equations. *Rev. Math. Phys.*, 20(6):625–706, 2008.

[11] Carlo Morosi and Livio Pizzocchero. An H^1 setting for the Navier-Stokes equations: quantitative estimates. *Nonlinear Anal., Theory Methods Appl., Ser. A, Theory Methods*, 74(6):2398–2414, 2011.

[12] Carlo Morosi and Livio Pizzocchero. On approximate solutions of the incompressible Euler and Navier-Stokes equations. *Nonlinear Anal., Theory Methods Appl., Ser. A, Theory Methods*, 75(4):2209–2235, 2012.

[13] Mitsuhiro T. Nakao and Kouji Hashimoto. A numerical verification method for solutions of nonlinear parabolic problems. *J. Math-for-Ind.*, 2009.

[14] Mitsuhiro T. Nakao, Takehiko Kinoshita, and Takuma Kimura. On a posteriori estimates of inverse operators for linear parabolic initial-boundary value problems. *Computing*, 94(2-4):151–162, 2012.

[15] Michael Plum. Existence and multiplicity proofs for semilinear elliptic boundary value problems by computer assistance. *Jahresber. Dtsch. Math.-Ver.*, 110(1):19–54, 2008.

[16] M. Raible, S. J. Linz, and P. Hänggi. Amorphous thin film growth: Minimal deposition equation. *Phys. Rev. E*, 62:1691–1694, 2000.

[17] James C. Robinson, Pedro Marín-Rubio, and Witold Sadowski. Solutions of the 3D Navier–Stokes equations for initial data in $\dot{H}^{\frac{1}{2}}$: robustness of regularity and numerical verification of regularity for bounded sets of initial data in $\dot{H}^1$. *J. Math. Anal. Appl.*, 400(1):76–85, 2013.

[18] M. Siegert and M. Plischke. Solid-on-solid models of molecular-beam epitaxy. *Physical Review E*, 50:917–931, 1994.

[19] Michael Winkler. Global solutions in higher dimensions to a fourth order parabolic equation modeling epitaxial thin film growth. *Zeitschrift für angewandte Mathematik und Physik*, 62(4):575–608, 2011.

[20] Piotr Zgliczyński. Rigorous numerics for dissipative PDEs. III: An effective algorithm for rigorous integration of dissipative PDEs. *Topol. Methods Nonlinear Anal.*, 36(2):197–262, 2010.